

Anisotropy of the probability of electron-phonon scattering in silver

V. A. Gasparov

Institute of Solid State Physics, USSR Academy of Sciences
(Submitted January 6, 1974)
Zh. Eksp. Teor. Fiz. 68, 2259-2270 (June 1975)

The shape and dimensions of the Fermi surface (FS) of silver are measured on the basis of the dependence of position of the radio-frequency size effect (RFSE) lines on the direction of the magnetic field. In this way the observed RFSE lines can be reliably identified. Values of electron-phonon collision frequencies averaged over the extreme orbits which form a dense screen enclosing the FS are obtained on the basis of measurements of the temperature dependence of the line amplitudes. From these data, the electron-phonon collision frequency, as a function of a point on the FS, is determined by mathematical inversion procedure using a computer. An experimental criterion for assessing the efficiency of electron-phonon collisions in metals is proposed.

PACS numbers: 71.30.Hr, 71.85.Ce

Experimental^[1, 2] and theoretical^[3, 4] investigations of the dependence of the frequency of electron phonon collisions $\nu = \tau^{-1}$ on the electron position on the Fermi surface (FS) of copper have revealed a strong anisotropy of the scattering probability. A study of other metals from this point of view, particularly silver, is of undisputed interest.

The measurements were made with the aid of the radio-frequency size effect (RSE). The positions of the RSE lines on closed trajectories relative to the magnetic field H_0 are determined by the extremal dimension k of the Fermi surface^[5]:

$$k = eH_0 d / 2\hbar c \quad (1)$$

(e is the electron charge, c is the speed of light, and d is the sample thickness), and the line amplitude is determined by the number of electrons of a narrow belt on the FS, near the extremal section, which have passed without scattering from one side of the plane-parallel sample to the other^[2]:

$$A \sim \exp(-2\pi\gamma\nu/\Omega), \quad (2)$$

where $\Omega = eH/mc$ is the frequency of the revolution of electrons having a cyclotron mass m in a magnetic field H , and γ is a geometric factor that determines within which part of the period $2\pi/\Omega$ the electrons traverse the distance between the two sides of the plate ($\gamma = 1/2$ for a circle). The collision frequency $\bar{\nu}$ is averaged over the points lying along the extremal orbit on the FS:

$$\bar{\nu} = \frac{\hbar}{2\pi m} \oint \frac{\nu(k) dk}{v_{\perp}(k)}; \quad (3)$$

here v_{\perp} is the projection of the Fermi velocity at the point k of the FS on the plane of the orbit.

An investigation of the dependence of the positions of the RSE lines on the direction of the magnetic field has made it possible to determine the shape and dimensions if the FS of silver and thus identify reliably the observed lines, while a study of the temperature dependences of the line amplitudes has made it possible to measure the value of $\bar{\nu}$ for the various orbits that form a dense network covering the FS, and to reconstruct in final analysis the frequency of the electron-phonon collisions as a function of the point on the FS.

EXPERIMENT

The RSE lines were drawn by determining the dependences of the derivative, with respect to the magnetic

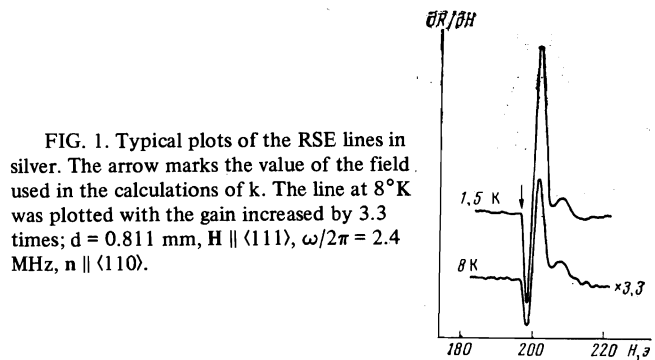


FIG. 1. Typical plots of the RSE lines in silver. The arrow marks the value of the field used in the calculations of k . The line at 8°K was plotted with the gain increased by 3.3 times; $d = 0.811$ mm, $H \parallel \langle 111 \rangle$, $\omega/2\pi = 2.4$ MHz, $n \parallel \langle 110 \rangle$.

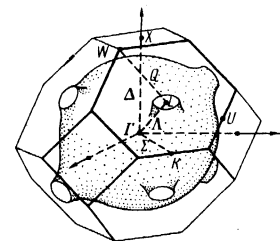


FIG. 2. Fermi surface of noble metals. [8].

field, of the active part of the sample surface impedance ($\partial R/\partial H$) in the frequency range 2 to 8 MHz and at temperatures 1.3 to 10°K. The methodological part of the experiments is described in^[2].

In investigations of the anisotropy of the extremal dimensions of the FS, the point from which one measures the positions of the lines recorded together with the NMR signal from the protons was chosen to be on the left edge of the lines (see Fig. 1).^[5] The error in the measurement of H_0 was 0.2%. The thickness was measured by a vertical optometer IZV-3 with accuracy $\pm 1 \times 10^{-4}$ cm, after which a correction was introduced for the shrinking of the cooled sample. The samples were plane-parallel within 0.3%, as a result of which the FS dimensions determined from were accurate to $\pm 0.5\%$. In the measurements, much attention was paid to the parallelism of the magnetic field to the sample surface, for even a very slight tilt of the field led to a broadening of the line and to a distortion of its shape.

The plane-parallel silver plates were cut from a single crystal and had a resistivity ratio $\rho(293^\circ\text{K})/\rho(4.2^\circ\text{K}) \approx 7 \times 10^3$. The samples were made smooth by mechanical

grinding on glass with M-10 silicon carbide powder. The cold-worked layer was removed by etching in the mixture used for chemical polishing.^[6] After a subsequent oxygen annealing^[7] for 10 hours, the resistivity ratio increased to 1.6×10^4 .

We investigated 9 samples with the normal n along $\langle 100 \rangle$, $\langle 110 \rangle$, and $\langle 121 \rangle$. The thickness ranged from 0.76 to 0.94 mm. In addition we prepared two samples with $n \parallel \langle 110 \rangle$ and thickness 0.2 mm to search for the lines from the neck of the FS.

THE FERMI SURFACE OF SILVER

The FS of noble metals is shown in Fig. 2. It is open along the $\langle 111 \rangle$ directions and occupies half the volume of the Brillouin zone. According to the free-electron model, the FS is a sphere fully inscribed inside the Brillouin zone, so that the presence of openings is a manifestation of interaction with the lattice potential.

Figure 3 shows the anisotropy of the extremal dimensions of the FS of silver in the planes $\{100\}$ and $\{110\}$, reconstructed from the experiment. It shows also the results of the de Haas-van Alphen effect.^[9] The ordinates represent the values of the wave vector k in units of the radius vector of the free-electron sphere ($k_{FE} = 1.2068 \text{ \AA}^{-1}$ at 4.2°K). In addition to the principal line due to the extremal sections with center at Γ , we observed lines due to chains of orbits with sections centered at X and L. All these sections have been investigated in the case of copper by Libchaber et al.^[10] and are not included in Fig. 3, since they provide only supplementary information. Even on the thinnest sample and at the minimal temperature 1.3°K we were unable to observe the SRE lines from the neck at $H \parallel \langle 111 \rangle$, whereas in copper it was reliably observed.^[2] The apparent reason for this is the maximal probability of electron scattering on the neck.

At $H \parallel \langle 121 \rangle$, the central-section electron orbit is open, and this leads to the appearance of a large number of RSE lines that are periodic in the magnetic field (Fig. 4). The period can be determined with good accuracy ($\pm 0.2\%$) from the recorded lines in a wide range of fields, so that it is possible to measure independently in this manner the thickness of the sample (the period of the opening in k -space is $2\Gamma L = 2.2161k_{FE}$). The thickness determined in this manner agrees well with the results of mechanical measurements.

The experimentally obtained anisotropy of the ex-

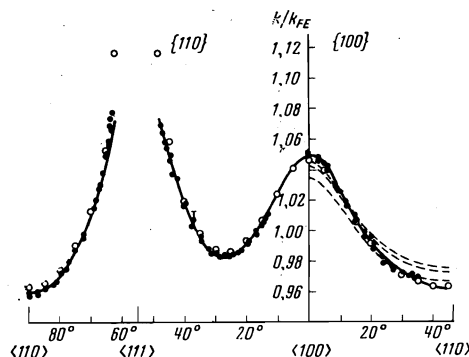


FIG. 3. Anisotropy of extremal dimensions of the FS of silver in the planes $\{100\}$ and $\{110\}$; ●—SRE, ○—de Haas-van Alphen effect.^[9] The dashed curves in plane $\{100\}$ are the results of Christensen's calculations at different values of E_F ,^[8] and the solid curve is a plot of the function (4).

FIG. 4. RSE lines on open orbit in silver. The lines in weak fields and between the main lines are due to open orbits (direction of opening parallel to the sample surface) and to chains of orbits (see insert); $d = 0.811 \text{ mm}$, $\omega/2\pi = 2.4 \text{ MHz}$, $H \parallel \langle 121 \rangle$, $n \parallel \langle 110 \rangle$.

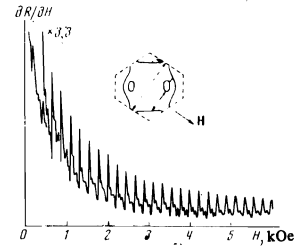


TABLE I. Dimensions of the FS of silver in units of k_{FE}

	Theory						Experiment		
	[8]	[9]	[9]	[9]	[9]	[9]	[9]	Present work	
k_X	0.142	0.230	1.108	1.086	0.095	1.130	1.0365	—	
$k_{\langle 100 \rangle}$	1.041	1.072	1.028	1.086	1.015	1.028	1.0469	1.07 ± 0.06	
$k_{\langle 110 \rangle}$	0.941	0.919	0.952	0.963	0.94	0.9713	0.9638	0.95 ± 0.01	
$k_{\langle 100 \rangle}/k_{\langle 110 \rangle}$	1.10	1.17	1.08	1.08	1.08	1.058	1.086	1.093	

Note. The presented data by Christensen^[8] were calculated using a different contribution of the exchange term.

tremal dimensions of the Fermi surface describes completely the intersections of the FS with the planes $\{110\}$ and $\{100\}$. The absence of experimental points at $H \parallel \langle 110 \rangle$ is due to the appearance of a "dog-bone" hole orbit with center at X (the corresponding dimensions are not given in Fig. 3) instead of a central section with center at Γ ; the corresponding RSE line is not seen in the $\{110\}$ plane, since the shape of the orbit is not favorable for the observation of the RSE.

Using for the radius vector of the FS an expansion in the cubic harmonics K_i ,^[11] we determined the expansion coefficients from the experimental anisotropy of the Fermi wave vector in the $\{100\}$ and $\{110\}$ planes by least squares with a computer. The sought function

$$k(\theta, \varphi) = (99.58 - 0.16K_1 + 1.63K_2 + 1.36K_3 - 0.53K_4 + 0.03K_5 + 0.29K_6) \cdot 10^{-2}k_{FE} \quad (4)$$

(k , θ , and φ are the spherical coordinates of a point on the FS) describes the anisotropy of the extremal dimensions of the FS with accuracy $\pm 0.5\%$ in the entire angle interval of the existence of the RSE lines. The error resulting from the use, in the calculation of the expansion coefficients, of the value of k on the neck, determined from the area of the section of the neck^[9] and from the dimensions of the Brillouin zone, was $\Delta k/k > 1\%$, owing to the strong anisotropy of the wave vector in this region. Nonetheless, expression (4), which describes the FS in the entire region except the neck itself, can be useful in a number of cases, since it makes it possible to determine the Fermi wave vector in a much simpler manner than by the use of the Fourier expansion.^[9]

As seen from Fig. 3, the measured dimensions of the FS agree within experimental accuracy with the data on the de Haas-van Alphen effect.^[9] At the same time, detailed investigations of the FS of copper, carried out with the aid of the RSE by Libchaber et al.,^[10] differ by 4.5% from the results obtained by other methods (ultrasound absorption, the de Haas-van Alphen effect).

Many papers have been devoted to calculations of the FS of noble metals from "first principles,"^[12] in spite of the extensive development of these methods, the results describe the shape and dimensions of the FS, but do not agree with experiment with sufficient accuracy (see Table I). The main obstacle here is apparently the uncertainty of the exchange term in the one-electron

potential. To get around these difficulties, Christensen^[8] calculated the FS of silver for three values of the Fermi level with different contributions of this term. As seen from Fig. 3, the theoretical results still do not make it possible to select a result that agrees best with experiment. Promising in this respect is the use of parametrization of the potential followed by fitting the parameters to the experimental data, as was done by Lee^[13] for copper with the aid of the "phase shift" method. Using only four parameters, agreement with experiment was attained within about 0.1%.

FREQUENCY OF ELECTRON-PHONON COLLISIONS

The conditions for the applicability of Eq. (2) were analyzed in^[2]. It was shown that the experimental criterion for the use of (2) is that the shape and width of the RSE lines remain constant in the investigated temperature interval. Indeed, in a paper by Wavner and Cochran,^[17] devoted to numerical calculations and experimental investigations of the RSE line shape in potassium, they obtained in the argument of the exponential of the line amplitude, in a transmission experiment, not the coefficient $\pi/2$,^[5] but a value 22% smaller:

$$A \sim e^{-1.22d/l}. \quad (5)$$

The calculations were made for the case $0.25d \leq l \leq 2d$ and $\delta = 0.035d$, where δ is the depth of the skin layer. Under these conditions, the appearance of, many revolutions and the appreciable change of l leads, as was in fact already demonstrated by Juras,^[18] to a change in the width and shape of the lines, and this is probably the cause of the unusual $A(l)$ dependence. At $l < 0.25d$, no detailed calculations were performed, but it was observed that the dependence in this case is stronger than (5). Under our conditions ($l \lesssim 0.25d$, $\delta \approx 0.003d$) the changes in the shape and width of the lines are negligibly small (see Fig. 1), and it appears that $\bar{\nu}(T)$ should be calculated with the aid of (2).

As seen from Fig. 5, in the entire investigated temperature interval the frequency $\bar{\nu}(T)$ is undoubtedly proportional to T^3 and consequently the cause of the scattering can be taken to be the electron-phonon interaction. The proportionality coefficient of T^3 depends essentially on the orientation of H . Figure 6 and Table II show the values of $\bar{\nu}(T)/T^3$ obtained for different samples (three in each plane), in different experiments, and at different frequencies. The scatter of the points about the mean value was $\lesssim 10\%$, which determines the measurement accuracy. The cyclotron masses in the planes {100} and

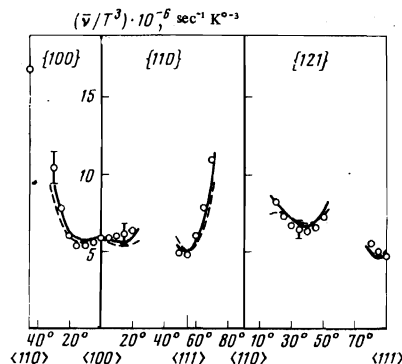


FIG. 6. The function $\bar{\nu}(H||H)/T^3$ for silver. The solid and dashed curves are explained in the text.

TABLE II

Plane {100} ($\varphi=0^\circ$)				Plane {110} ($\varphi=45^\circ$)				Plane {121}				
N ₀	θ , deg	m/m_0	$\bar{\nu}/T^3$	N ₀	θ , deg	m/m_0	$\bar{\nu}/T^3$	N ₀	θ , deg	φ , deg	m/m_0	$\bar{\nu}/T^3$
1	0	0.93	5.9	8	0	0.93	5.9	18	54.7	45	0.93	4.9
2	5	0.93	5.5	9	5	0.93	5.5	19	54.9	38.9	0.92	5.0
3	10	0.93	5.4	10	10	0.93	6.2	20	55.3	32.8	0.92	5.5
4	15	0.94	5.4	11	15	0.93	6.2	21	63.7	89.2	0.99	7.2
5	20	0.95	6.1	12	20	0.93	6.4	22	65.9	84.2	0.96	6.5
6	25	0.96	8.1	13	25	0.95	4.9	23	68.2	79.4	0.95	6.3
7	30	1.03	10.5	14	30	0.93	4.8	24	70.6	74.7	0.97	6.4
28	45	1.03	16.8	15	35	0.93	6.0	25	73.2	70.3	0.99	6.6
				16	40	0.98	7.9	26	75.8	65.8	1.03	7.3
				17	45	1.03	11.0	27	78.6	61.5	1.04	8.2

Note. The collision frequency $\bar{\nu}/T^3$ is expressed in units of $10^6 \text{ sec}^{-1} \text{ K}^{-3}$. θ and φ are the spherical coordinates of the direction of H . The orbits 1, 8, 14, and 18 correspond to one and the same direction of H : 1 and 8 to $H || \langle 100 \rangle$ and 14 and 18 to $H || \langle 111 \rangle$. The orbit 28 is known in the literature as the "dog-bone" orbit.

{110} were taken from Howard's paper,^[19] and in the plane {121} from our calculations (see below).

EFFECTIVENESS OF ELECTRON-PHONON COLLISIONS

Formula (3) differs from that used for copper in the absence of a weighting factor $|\cos \psi|$, where ψ is the angle between the electron velocity and the normal to the sample surface. It is possible to dispense with this function by performing the measurements under conditions when the scattering angle q/k_F ($q = k_B T / \hbar s$ is the wave vector of the phonon, k_B is Boltzmann's constant and s is the speed of sound) is larger than the maximum dimension of this region on the FS, where the increment to the distribution function differs from zero: $q/k_F > (\delta/d)^{1/2}$.^[24] To compare the effectiveness of scattering in different metals on that part of the orbit where $\mathbf{v} \perp \mathbf{n}$, we can use the parameter $\eta = (k_B T d^{1/2} / \hbar k_F s \delta^{1/2})$. The values of η for different metals, determined from the depth δ of the skin layer ($\delta/d = 0.15 \Delta H / H$ ^[26]) and referred to the midpoint of the investigated temperature interval, are respectively: 0.08 (Tl^[20], Cd^[21, 22]); 0.12 (In^[23]); 0.15–0.08 (K^[24]); 0.15 (Sn^[25], Cu^[2]); 0.25 (Ag—the present paper).

It is difficult to indicate beforehand the exact value of this parameter that serves as the demarcation point between the effective and ineffective scattering; it is only clear that it is close to unity. Therefore, trying to make η as large as possible, we used for the degree of effectiveness an experimental criterion based on the temperature dependences of the amplitudes of the RSE lines on trajectory chains.

In the case of RSE on chains of two, three, etc. links

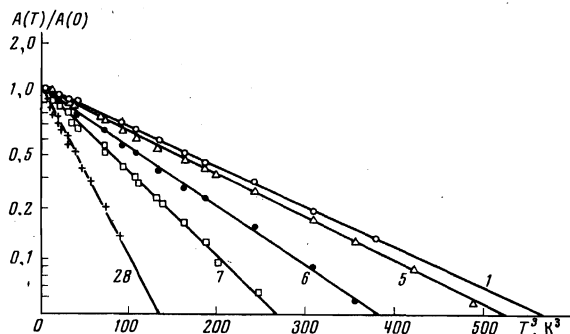


FIG. 5. Temperature dependence of the amplitudes of the SRE lines for a silver sample at different directions of the magnetic field in the sample plane (see Table II); $d = 0.933 \text{ mm}$, $\omega/2\pi = 4.5 \text{ MHz}$, $\mathbf{n} || \langle 100 \rangle$.

we have $\eta \sim n^{1/2}$ (n is the number of orbits within the thickness of the sample), inasmuch as it is necessary to replace d in η by the electron orbit diameter 2 . Under ideal conditions, when $\eta \gg 1$ and the multiple revolutions play no role, we have $A_n(T)/A_n(0) = A_1(T)/A_1(0)$, since the intensity of the RSE line is proportional to the n -th power of the amplitude in the first burst, i.e., $A_n \sim [\exp(-2\pi mc\gamma/enH_1)\bar{\nu}]^{n!}$. To the contrary, investigations of $A_n(T)/A_n(0)$ in potassium, by Tsoi and Gantmakher,^[24] under conditions $\eta \approx 0.1$, have shown that for lines with n equal to 2 or 3 the coefficient of T^3 is smaller by a factor of two and three, respectively, than for $A_1(T)/A_1(0)$. Measurements of $A_n(T)$ in thallium ($\eta \approx 0.08$), carried out by Bradfield and Coon^[20], have revealed so strong a change of effectiveness for high-number lines, that a transition occurred from the T^3 dependence to a T^4 dependence. At the same time, halving the sample thickness^[24], which is equivalent to a transition to a line in a field $2H_1$ for a thick sample, did not affect the coefficient of T^3 , in spite of the fact that it was accompanied by a transition from the condition $\delta/d \lesssim q/k_F$ to $\delta/d \gtrsim q/k_F$. It is possible that this circumstance is due to the appearance of multiple turns in thin samples, which should affect in the same manner higher-number lines of thick samples. In the case of a chain of orbits, however, the contribution of a total orbit ($\gamma = 1$) in comparison with its half ($\gamma = 1/2$) is small, since the electron acquires a small increment to the distribution function on passing through the "interior" skin layer (the amplitude of the field in the first and succeeding bursts decreases strongly in comparison with the surface burst^[27]). Therefore an important role is played by the orbits with $\gamma = 1/2, 3/2, \dots$ whereas contributions to the formation of the RSE line in the field H_1 is made by the orbits with $\gamma = 1/2, 2/2$, etc.

On the other hand, the numerical calculations by Wagner and Cochran^[17] of the RSE line shape in potassium in a field $2H_1$, made under the assumption that each scattering act is effective (this assumption is incorrect for electron-phonon interactions under the considered conditions), have revealed that $A_2(l)$ varies in accordance with the exponential law (5), but in which the argument of the exponential is 30% smaller. This difference between $A_1(l)$ and $A_2(l)$ is apparently due to the causes referred to above in the discussion of the applicability of formula (2). At the same time, the argument of the exponential in the experimental^[17] $A_2(T)$ dependence turned out to be 80% smaller than for $A_1(T)$, in agreement with our assumption that the electron-phonon collisions are less effective for lines with $n > 1$.

Thus, the temperature dependence of the RSE line amplitudes in multiple fields can serve as a test for an estimate of the collision effectiveness. Figure 7 shows plots of the RSE effect in silver at $H \parallel \langle 100 \rangle$. At other field orientations, the observation of lines with $n > 1$ is made difficult by the presence of lines due to orbits with center in L , and also by orbits passing through several repeating Brillouin zones.

As seen from Fig. 8a, in silver the condition for effectiveness is satisfied with some margin, since the temperature dependence of the line amplitude in a double field is the same as for the first line, and the averaging (3) can therefore be used. Only on going to lines with $n = 3$ and 4 is a decrease observed in the coefficient of T^3 , in accord with the arguments presented above. For a comparison with copper, Fig. 8b shows that in copper,

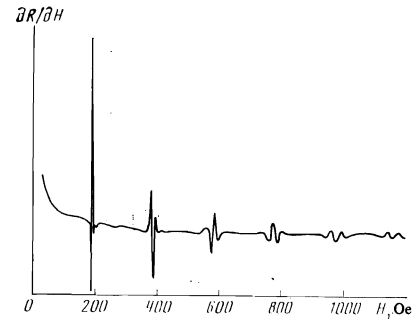


FIG. 7. RSE lines on chains of orbits in a silver sample; $d = 0.805$ mm, $T = 4.2^\circ\text{K}$, $\omega/2\pi = 2.2$ MHz, $n \parallel \langle 110 \rangle$, $H \parallel \langle 100 \rangle$.

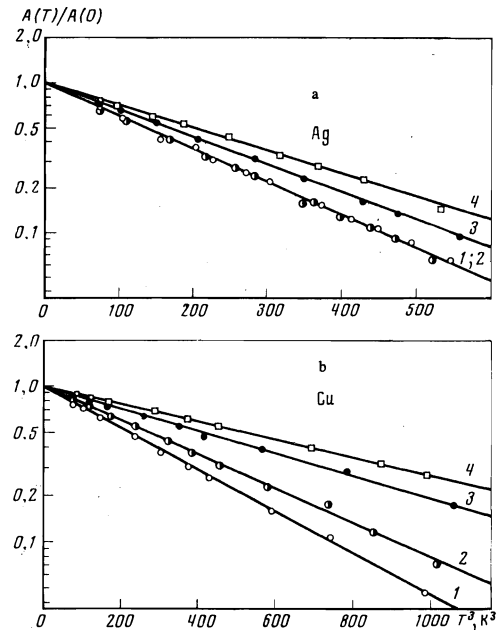


FIG. 8. Temperature dependence of the amplitudes of RSE lines in silver (see Fig. 7) and copper ($d = 0.71$ mm, conditions the same as in the silver). The plots are labeled by the numbers of the chains in the orbits. The points \circ and \bullet pertain to the lines $n = 1$ and $n = 2$, respectively.

under the investigated conditions, the coefficient of T^3 is smaller already at $n = 2$ than on the line with $n = 1$, thus confirming the conclusion drawn in^[2] that electron-phonon collisions differ in their effectiveness at different points of the orbit.

REDUCTION OF THE RESULTS

The end result of the investigations is the frequency of the electron-phonon collisions as a function of the point on the FS. To reconstruct this function from the experimental $\bar{\nu}(H/H_1)$ relation, we used the mathematical procedure described in^[2]. The local frequency of the electron phonon collisions $\nu(\mathbf{k})$ was expanded in a three-dimensional Fourier series

$$\nu(\mathbf{k}) = T^3 \sum_{i=1}^l w_i F_i(\mathbf{k}), \quad (6)$$

where w_i are expansion coefficients to be determined and $F_i(\mathbf{k})$ are Fourier-series terms having cubic symmetry:

$$F_{lmn}(\mathbf{k}) = \sum \cos\left(\frac{lak_x}{2}\right) \cos\left(\frac{nak_y}{2}\right) \cos\left(\frac{mak_z}{2}\right) \quad (7)$$

($l+n+m = 0, 2, 4, \dots$, a is the lattice parameter, the summation is over the permutations of the indices x ,

y, and z). After substituting (6) in (3) and determining with a computer the integrals over the central sections of the FS $\Psi(\mathbf{k}) = 0$ (using the Halse data^[9] on the anisotropy of the Fermi momentum and the electron velocity):

$$a_{ij} = \frac{\hbar}{2\pi m_j} \int_0^{2\pi} \frac{k^2 F_{ij} |\nabla \Psi| d\xi}{(k, \nabla \Psi) |v|} \quad (8)$$

(ξ is the polar angle on the j -th extremal orbit), the problem of determining $\nu(\mathbf{k})$ is reduced to a solution of a system of p algebraic equations

$$\bar{\nu}_j/T^3 = \sum_i a_{ij} w_i; \quad i=1, 2, \dots, t, \quad j=1, 2, \dots, p \quad (9)$$

with t unknowns. The number p is equal to the number of employed experimental points, and t was increased until the deviation of the experimental values from the function $\bar{\nu}(H/|H|)$ obtained by least squares with the computer did not exceed 10%. Calculation of the integral in (8) at $F_1 = 1$ has made it possible to determine the effective mass and by the same token served as a check on the calculation.

The diameter of the neck in silver is smaller by a factor 1.4 than in copper, and therefore the orbits in the planes $\{100\}$ and $\{110\}$ cover a larger part of the Fermi surface than in copper.^[2] Furthermore, the additional use of the $\{121\}$ plane has made it possible to increase the number of investigated orbits to 26 and the number of the expansion terms t to five. While further increase of t does decrease the rms error, the resultant function $\nu(\mathbf{k})$ is no longer smooth.

The sought function

$$\nu(\mathbf{k})/T^3 = -(23.13 + 63.25F_{110} + 10.29F_{200} + 8.16F_{211} + 2.44F_{220}) \times 10^7, \text{ sec}^{-1} \cdot \text{K}^{-3} \quad (10)$$

is shown in Figs. 9 and 10 and agrees better with the experimental values than all other employed functions. To estimate the accuracy of the inversion procedure, the dashed curve in Fig. 6 is a plot of the function $\bar{\nu}(H/|H|)$ exceeding the 10% experimental error. This function was obtained from the calculated function by random variation of the expansion coefficients. It is seen that the solution (10) (solid curve) is stable, since a small change of $\bar{\nu}(H/|H|)$ leads to small changes of $\nu(\mathbf{k})$ (dashed curve in Fig. 9).

Even though the region near the neck was excluded from consideration (the "dog-bone" orbit was not included in the calculations) and there is no experimental value of $\bar{\nu}$ on the neck, the function $\nu(\mathbf{k})$ near the neck

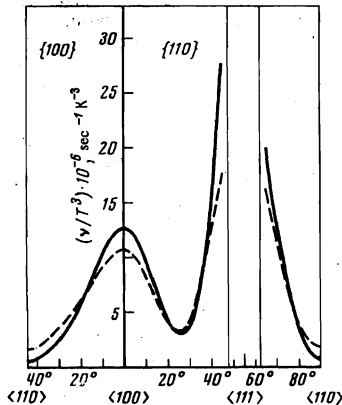


FIG. 9. The function $\nu(\mathbf{k})/T^3$ in silver in the planes $\{100\}$ and $\{110\}$. The vertical lines mark the boundaries of the neck, and the dashed curve is explained in the text.

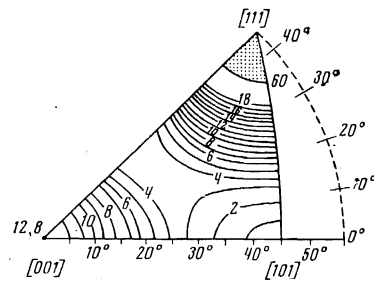


FIG. 10. Stereographic projection of the lines $\nu(\mathbf{k})/T^3 = \text{const}$ (the function (10) in units of $10^8 \text{ sec}^{-1} \text{ K}^{-3}$) on $1/48$ -th of the FS of silver.

reveals a sharp maximum, which is the result of the inversion of the experimental data. Nonetheless, the function (10) has not been continued in Figs. 9 and 10 to the boundaries of the neck, since the orbits used in the calculations do not go through the neck and yield no information on the behavior of the collision frequency on this section of the FS. However, the value of $\nu(\mathbf{k})$ on the neck was nevertheless determined in the following manner: the function (10) was terminated at angles 3° from the neck boundary (see Fig. 9), and was subsequently extrapolated linearly towards the value of $\nu(\mathbf{k})$ on the neck, which was used as a variable parameter. The value of $\bar{\nu}$ was then calculated by numerical integration in accordance with formula (3) and compared with the experimental value on the orbit (28) ("dog-bone"). The best agreement was obtained at $\nu_N/T^3 = 60 \times 10^8 \text{ sec}^{-1} \text{ K}^{-3}$.

DISCUSSION

The functions $\nu(\mathbf{k})$ in copper^[2] and in silver turned out to be quite close (cf. Fig. 9 and Fig. 4 of^[2]), except for the region of the neck. If we estimate the ratio $\nu_{\text{Ag}}(\mathbf{k})/\nu_{\text{Cu}}(\mathbf{k})$ by using the relation^[2]

$$\nu(\mathbf{k}) = \frac{3.6}{\pi} \frac{\Delta^2 (k_B T)^2}{\hbar^2 s^4 \mu v} \quad (11)$$

(Δ is the constant of the deformation potential and μ is the density), then it turns out that equality of the electron-phonon collision frequencies in these metals is the consequence of the smallness of the deformation potential in silver, $\Delta_{\text{Cu}} \approx 1.3 \Delta_{\text{Ag}}$. A similar result follows from a comparison of the parameters of the electron-phonon renormalization $\lambda(\mathbf{k}, T)$ in these metals.

The value of this parameter in the low-temperature limit^[28]

$$\lambda(\mathbf{k}, 0) = \frac{2}{(2\pi)^3} \sum_{\sigma} \int \frac{dS_{\mathbf{k}'} |M_{\sigma}(\mathbf{k}, \mathbf{k}')|^2}{\hbar v_{\mathbf{k}'} \hbar \omega_{\mathbf{k}-\mathbf{k}', \sigma}} \quad (12)$$

(the summation is over all phonon polarizations σ , the integration is over the FS, ω is the phonon frequency), just as the frequency of the electron-phonon collisions

$$\nu(\mathbf{k}) = \frac{2}{(2\pi)^3} \frac{1}{\hbar} \sum_{\sigma} \int \frac{dS_{\mathbf{k}'} |M_{\sigma}(\mathbf{k}, \mathbf{k}')|^2}{\hbar v_{\mathbf{k}'} \text{sh}(\hbar \omega_{\mathbf{k}-\mathbf{k}', \sigma} / k_B T)} \quad (13)$$

is proportional to the square of the matrix element of the electron-phonon interaction $M_{\sigma}^2(\mathbf{k}, \mathbf{k}')$ which transfers the electron from the state \mathbf{k} to the state \mathbf{k}' . The values of $\lambda(\mathbf{k}, 0)$ are determined by comparing the experimental and theoretical Fermi velocities $\nu(\mathbf{k})$ and $\nu_0(\mathbf{k})$ respectively:

$$\nu(\mathbf{k}) = \nu_0(\mathbf{k}) / [1 + \lambda(\mathbf{k}, 0)]. \quad (14)$$

In copper^[28], $\lambda(\mathbf{k}, 0)$ is a strongly anisotropic function that duplicates the anisotropy of $\nu(\mathbf{k})$ in accord with formulas (12) and (13): $\lambda = 0.211$ along $\langle 100 \rangle$ and

$\lambda = 0.038$ along $\langle 110 \rangle$. At the same time the value of $\lambda(\mathbf{k}, 0)$ is quite small (0.00 ± 0.01) or is even negative along certain directions,^[8] which generally speaking is physically meaningless and is apparently due to the inaccuracy of the band-spectrum calculation. The smallness of $\lambda(\mathbf{k}, 0)$ in silver is probably the result of the smallness of M^2 , so that it can be assumed that despite the large phonon momentum the collision frequency in silver is the same as in copper, owing to the smallness of the electron-phonon interaction matrix.

The observed dependence of the collision probability on the position of the electrons on the FS is determined by the anisotropy of several parameters: the phonon spectrum, the state density, the electron wave functions, and the deformation potential. It is therefore difficult to point out the main factor governing the function $\nu(\mathbf{k})$, and theoretical calculations of the function $\nu(\mathbf{k})$ are needed, with due allowance for the anisotropy of all these parameters, similar to what was already done for copper.^[3, 4]

In conclusion, the author thanks V. F. Gantmakher for discussions and critical remarks, L. G. Fedyaeva for help with the computer calculations, R. N. Nikolaev and N. V. Lichkova for supplying the pure silver single crystal, and M. A. Arutyunyan for help with the experiments.

¹R. E. Doezema and J. F. Koch, Phys. Rev., B6, 2071 (1972).

²V. F. Gantmakher and V. A. Gasparov, Zh. Eksp. Teor. Fiz. 64, 1712 (1973) [Sov. Phys.-JETP 37, 864 (1973)].

³D. Nowak, Phys. Rev., B6, 3691 (1972).

⁴Sh. G. Dass, Phys. Rev., B7, 2238 (1973).

⁵V. F. Gantmakher, Progr. in Low Temp. Phys. ed. Gorter C. J., Amsterdam, North Holland, 51, 181 (1967)

⁶J. O. Henningsen, Phys. Status Sol., 32, 239 (1969).

⁷J. O. Henningsen, Phys. Lett., 27A, 693 (1968).

⁸N. E. Christensen, Int. reprint Physics Labor. I, The Technical University of Denmark, Lyngby, 1970.

⁹M. R. Halse, Phil. Trans. Roy. Soc., 265, 507 (1969).

¹⁰B. Perrin, G. Weisbuch, A. Libchaber, Phys. Rev., B1, 1501 (1970).

¹¹M. J. G. Lee, and L. M. Falicov, Proc. Roy. Soc., A304, 319 (1968).

¹²J. O. Dimmock, Sol. St. Phys., 26, 103 (1971) ed. H. Ehrenreich, F. Seitz and D. Turnbull (New York; Acad. Press).

¹³M. J. G. Lee, Phys. Rev., 187, 904 (1969).

¹⁴E. C. Snow, Phys. Rev., 172, 708 (1968).

¹⁵W. J. O'Sullivan, A. C. Switendick and J. E. Schirber, Phys. Rev., B1, 1443 (1970).

¹⁶H. V. Bohm and V. J. Easterling, Phys. Rev., 128, 1026 (1962).

¹⁷D. K. Wagner and R. Cochran, The Mat. Sci. Cent. Cornell Univ., reprint 2259, 1974.

¹⁸G. E. Juras, Phys. Rev., 187, 784 (1969).

¹⁹D. G. Howard, Phys. Rev., 140, 1705 (1965).

²⁰J. E. Bradfield and J. B. Coon, Phys. Rev., B7, 5072 (1973).

²¹V. P. Nabereznykh and L. T. Tsymbal, ZhETF Pis. Red. 5, 319 (1967) [JETP Lett. 5, 263 (1967)].

²²S. B. Soffer, R. Huguenin and P. A. Probst, J. Low Temp. Phys., 11, 537 (1973).

²³I. P. Krylov and V. F. Gantmakher, Zh. Eksp. Teor. Fiz. 51, 740 (1966) [Sov. Phys.-JETP 24, 492 (1967)].

²⁴V. S. Tsoř and V. F. Gantmakher, Zh. Eksp. Teor. Fiz. 58, 1232 (1969) [Sov. Phys.-JETP 29, 663 (1969)].

²⁵V. F. Gantmakher and Yu. V. Sharvin, Zh. Eksp. Teor. Fiz. 48, 1077 (1965) [Sov. Phys.-JETP 21, 720 (1965)].

²⁶E. A. Kaner. Physics, 3, 301 (1967).

²⁷E. A. Kaner, Zh. Eksp. Teor. Fiz. 44, 1036 (1963) [Sov. Phys.-JETP 17, 700 (1963)].

²⁸M. J. G. Lee, Phys. Rev., B2, 250 (1970).

Translated by J. G. Adashko

240